^{1}H MR Spectroscopy of the Brain: Absolute Quantification of Metabolites[1]

Jacobus F. A. Jansen, MS
Walter H. Backes, PhD
Klaas Nicolay, PhD
M. Eline Kooi, PhD

Hydrogen 1 (^{1}H) magnetic resonance (MR) spectroscopy enables noninvasive in vivo quantification of metabolite concentrations in the brain. Currently, metabolite concentrations are most often presented as ratios (eg, relative to creatine) rather than as absolute concentrations. Despite the success of this approach, it has recently been suggested that relative quantification may introduce substantial errors and can lead to misinterpretation of spectral data and to erroneous metabolite values. The present review discusses relevant methods to obtain absolute metabolite concentrations with a clinical MR system by using single-voxel spectroscopy or chemical shift imaging. Important methodological aspects in an absolute quantification strategy are addressed, including radiofrequency coil properties, calibration procedures, spectral fitting methods, cerebrospinal fluid content correction, macromolecule suppression, and spectral editing. Techniques to obtain absolute concentrations are now available and can be successfully applied in clinical practice. Although the present review is focused on ^{1}H MR spectroscopy of the brain, a large part of the methodology described can be applied to other tissues as well.

[1] From the Department of Radiology, Maastricht University Hospital, P. Debyelaan 25, 6202 AZ Maastricht, the Netherlands; and Biomedical NMR, Department of Biomedical Engineering, Eindhoven University of Technology, Eindhoven, the Netherlands.

Address correspondence to J.F.A.J. (e-mail: *j.f.a.jansen@tue.nl*).

Radiology

Hydrogen 1 (^{1}H) magnetic resonance (MR) spectroscopy enables noninvasive quantification of in vivo metabolite concentrations in the brain. It has proved to be a powerful addition to the clinical assessment tools for numerous pathologic conditions, including epilepsy, multiple sclerosis, stroke, cancer, and metabolic diseases (1).

In nuclear MR, the total area under a metabolite resonance in a ^{1}H MR spectrum is directly proportional to the concentration of the metabolite. Currently, metabolite concentrations are usually expressed as ratios (relative quantification) rather than as absolute concentrations. Ratios can be useful for clinical diagnosis to characterize pathologic tissue. For example, relative quantification has been successfully applied in the diagnosis of cancer (2), leukemia (3), epilepsy (4), dementia (5), and multiple sclerosis (6). A locally obtained reference data set with normal ratios for healthy tissue can be used for most clinical purposes, while for focal pathologic conditions a reference spectrum can be acquired from the contralateral region of the patient's brain. The use of signal ratios has the great advantage that it is very easy to implement because it does not require extra imaging time and time-consuming postprocessing. Furthermore, a number of problems—for example, partial volume effects arising from different amounts of cerebrospinal fluid in the selected volumes—can be largely avoided. In addition, ratios are, in some cases, more sensitive in terms of detecting changes (eg, when one metabolite increases and another decreases) and can be more accurate than absolute concentrations, owing to specific characteristics of the analysis computer program applied (7).

If a change is observed in the ratio of metabolite peaks, however, it remains uncertain which metabolite concentration actually changes. This information can only be obtained from absolute concentrations. Absolute quantification (AQ, also referred to as absolute quantitation) implies that concentrations are expressed in biochemical units, such as millimoles per kilogram wet weight. Furthermore, when spectroscopic results are to be compared in an interdisciplinary context (eg, with biochemically derived concentrations), ratios or arbitrary units might not be appropriate.

Since many factors need to be considered to obtain reliable absolute concentrations with ^{1}H MR spectroscopy, it is hard for a newcomer to comprehend all aspects and potential pitfalls concerned with AQ and to decide which method to use. The latest reviews on AQ were written several years ago (8–11), when AQ was more or less considered to be a basic research tool. However, several groups have recently published clinical trials that incorporate AQ. These include studies of patients with Alzheimer disease (12), epilepsy (13–15), multiple sclerosis (16,17), leukoencephalopathy (18), amyotrophic lateral sclerosis (19), and cancer (20). Furthermore, the reviews published so far have mainly focused on single-voxel spectroscopy, whereas spectra simultaneously recorded from multiple adjoining spatial regions (chemical shift imaging) find increasing use in many clinical trials (13,15,17,21). In addition, new developments, such as spectral editing, macromolecule suppression, tissue segmentation, and quantitative analysis of spectra with dedicated software, can aid in AQ of brain metabolites. This review will address the implementation of these new developments in AQ strategies.

Essentials

- Although metabolite ratios can be useful, absolute quantification (AQ) has an added value, since concentrations obtained through AQ procedures benefit from unambiguous interpretation and may be less prone to error.
- The AQ procedure is divided into two steps: *(a)* determination of accurate peak areas for the relevant metabolites and *(b)* conversion of peak areas into metabolite concentrations by using a calibration procedure.
- The implementation of AQ has been greatly facilitated by the development of calibration strategies and the availability of spectral fitting routines.
- AQ is available and can improve the diagnostic utility of ^{1}H MR spectroscopy.
- AQ requires more time and expertise than does relative quantification, and one can only benefit from AQ if all additional reference steps are executed properly; otherwise, unwanted additional errors may be introduced.

Advantages and Disadvantages of Absolute Metabolite Concentrations

In relative quantification, which yields concentrations expressed as ratios, one of the metabolite peaks measured is used as the concentration standard and serves as the denominator of the peak ratios. As a result, the total number of quantifiable metabolites is decreased by one. Furthermore, alterations in the peak ratio do not necessarily reflect a change in the concentration of the numerator. The alteration may be caused by changes in the concentration of the numerator, the denominator, or both or may merely be due to changes in relaxation behavior.

The assumption that the concentration of certain reference metabolites (eg, total creatine, choline) remains constant may be incorrect under normal conditions, as well as in many pathologic states. For example, it has been shown in patients with temporal lobe epilepsy (22) that the temporal lobe ipsilateral to the seizure focus displays a significant increase in total creatine and choline; a similar finding has also been reported in patients with frontal lobe epilepsy (23). Furthermore, even the temporal lobe contralateral to the sei-

Published online
10.1148/radiol.2402050314

Radiology 2006; 240:318–332

Abbreviations:
AQ = absolute quantification
NAA = *N*-acetylaspartate
RF = radiofrequency
SNR = signal-to-noise ratio
VOI = volume of interest

zure focus exhibits total creatine and choline concentrations that are increased, albeit not significantly (22). In addition, if patients have global metabolic defects, comparisons with contralateral brain regions (which are assumed to be metabolically normal) may not be feasible (24,25).

Clear evidence has recently been provided showing that, in addition to causing possibly ambiguous interpretation, relative quantification may introduce larger errors than does AQ (26,27). Two independent ^{1}H MR spectroscopy studies with healthy volunteers in whom single-voxel spectroscopy (27) and chemical shift imaging (26) were used have shown that metabolite ratios exhibit higher coefficients of variation (up to 1.6-fold) than do AQ concentrations of individual metabolites. Furthermore, authors of a chemical shift imaging study in patients with temporal lobe epilepsy (15) reported that metabolite ratios were less sensitive to abnormalities than were absolute values. It is, therefore, advisable to obtain concentrations expressed in standard units (such as millimoles per kilogram wet weight) by applying AQ. One should realize, however, that AQ requires more time than does relative quantification, and one can benefit from AQ only if all additional referencing steps are executed properly; otherwise, unwanted additional errors may be introduced.

Theoretic Background

Characteristics of the Radiofrequency Coil

Radiofrequency (RF) coils are used to transmit the RF magnetic induction field (B_1) and to detect the resulting signal. In the case of clinical ^{1}H MR spectroscopy of the brain, the patient's head is positioned within the head coil, which is used as a receive coil, while either the head or the body coil acts as the transmit coil. With a dedicated pulse sequence such as point-resolved spatially localized spectroscopy, or PRESS (28), or stimulated-echo acquisition mode, or STEAM (29), a spectrum can be obtained from a single well-defined spatial volume (single-voxel spectroscopy) to demonstrate metabolites. Alternatively, multiple spectra can be obtained simultaneously from multiple adjoining spatial regions (chemical shift imaging, also referred to as MR spectroscopic imaging) (30,31). The transmit coil should generate RF pulses with sufficient power to penetrate into all tissue regions of interest.

The requirements for signal reception are generally similar to those for transmission. The penetration of the RF pulses of the transmit coil and the signal-to-noise ratio (SNR) from the receive coil are strongly dependent on the coil loading, which is determined by the electric conductivity of the coil and the volume of the object near the coil. Variations in the size and tissue composition of the head positioned in the RF coil affect the amount of RF energy that gets into and the amount of signal detected from the volume of interest (VOI). This is one of the reasons why the electric characteristics of the RF coil are optimized before measurement begins, to achieve the most efficient performance.

Characteristics of MR Spectra

A water-suppressed brain ^{1}H MR spectrum typically displays a number of signals that correspond to several brain metabolites. These signals are characterized by one or more peaks with a certain resonance frequency, line width (full width at half maximum of the peak's height), line shape (eg, lorentzian or Gaussian), phase, and area. The peaks are separated owing to differences in resonance frequency, which are caused by the difference in the chemical environment of the different nuclei. The molecular structure of a particular metabolite is reflected by a typical peak pattern. The area of a peak is directly proportional to the number of nuclei that contribute to it and to the concentration of the metabolite to which the nuclei belong. However, the peak areas are also influenced by other factors, including T1 and T2 relaxation times.

Quantification of ^{1}H MR Spectra

Generally, the quantification procedure is divided into two steps. In the first step, accurate peak areas for the relevant metabolites are determined. In the second step, careful calibration is used to convert peak areas to metabolite concentrations to which the metabolite signals are referenced.

Definitions of Concentration

Different quantification strategies lead to different concentration standards. Two definitions of concentration are commonly used: *(a)* molarity, which is the number of moles of metabolite per liter of tissue water, and *(b)* molality, which is the number of moles of metabolite per kilogram of tissue water. In principle, molal concentrations can be converted into molar concentrations (32) by using a conversion that requires knowledge of the specific brain tissue density.

Comparison of in Vivo ^{1}H MR Spectroscopy to Other Quantification Methods

Most alternative quantification methods can only be performed in vitro, after brain autopsy. These methods include high-pressure liquid chromatography and high-field-strength (>7-T) ^{1}H MR spectroscopy. Whereas in vivo ^{1}H MR spectroscopy can only determine metabolites with a concentration on the order of millimoles, both high-pressure liquid chromatography and high-field-strength ^{1}H MR spectroscopy can demonstrate concentrations in the micromolar range. However, several metabolites, including *N*-acetylaspartate (NAA) and phosphocreatine, are generally detected at lower concentrations by using in vitro methods (up to 10% reduction relative to that detected in vivo in healthy subjects) (33,34) owing to the rapid degradation of these metabolites in brain tissue samples immediately after autopsy (35,36). The assessment of metabolites that are not subject to degradation yields similar concentrations in both in vivo and in vitro methods (37). Typical metabolite concentrations in parietal lobe white matter obtained with in vivo ^{1}H MR spectroscopy are 9.6 mmol per kilogram (mmol/kg) wet weight ± 3.0 (standard deviation) for NAA, 7.0 mmol/kg wet weight ± 2.0 for total cre-

atine, 1.8 mmol/kg wet weight ± 0.5 for choline, and 5.2 mmol/kg wet weight ± 3.3 for *myo*-inositol (38).

Quantification Strategies

In this section, the most widely used quantification strategies for in vivo ^{1}H MR spectroscopy are described. The relative merits and drawbacks of each approach are indicated in Table 1. The schematic setup for the brain and calibration measurement for each case is shown in Figure 1.

Relative Quantification Method

One of the simplest approaches is the internal endogenous marker method. With this approach, one of the measured peaks, originating from an endogenous metabolite, serves as a concentration standard (Fig 1, *A*). Peak ratios (possibly corrected for factors such as relaxation) are converted into concentrations by using a value from the literature for the reference metabolite, whose concentration is supposed to be invariant. Commonly used reference metabolites are NAA, total creatine, and choline. Although this method allows direct comparison with other biochemical measurements, it is essentially a relative quantification method and shares all previously mentioned possible merits and drawbacks.

AQ Methods

External reference method.—A vial with a known reference solution and relaxation properties is positioned near or inside the RF coil (Fig 1, *B*) (39). Immediately after the acquisition of the in vivo spectrum, a reference spectrum from the calibration sample is obtained while the patient's head is still inside the coil. The reference spectrum can also be obtained simultaneously with the acquisition of patient data (40). An option to account for possible B_1 inhomogeneity is to measure (41) or to simulate (42) the B_1 distribution of the RF coil used. It is important to realize that the external vial might introduce substantial distortions of the constant magnetic induction field (B_0) homogeneity, which will complicate shimming (adjustment of the homogeneity of the local magnetic field) and water suppression.

Replace-and-match method.—The basic principle of the replace-and-match strategy is to replace the human subject with a phantom that simulates (human) tissue as closely as possible and to match the coil load to the load obtained previously in vivo (Fig 1, *C*) (43,44). Then, a calibration measurement is performed, which is identical with respect to all imager settings (eg, pulse sequence and size and position of the VOI). The phantom usually contains a solution that mimics the electric conductivity of human tissue. Fine adjustment of the coil load can be made by placing the phantom further inside or outside the coil or by inserting a small bottle containing saline. It is important that the load be accurately matched, because it is usually not possible to eliminate the effect of a difference in load by using a post hoc correction factor (44). Unfortunately, the matching of the load by maneuvering the phantom is not always straightforward and can be time consuming. Furthermore, the B_1 distribution through a phantom is often con-

Table 1

Relative Merits and Drawbacks of Quantification Strategies

Strategy	Extra Imaging Time for Examination	Extra Imaging Time after Examination	Preparation Time†	Ease of Use	Accuracy
Internal endogenous marker	+	+	+	+	−
External reference	−	+	0	−	0
Replace-and-match method	+	−	−	−	+
Water signal reference	−	+	+	0	0
Principle of reciprocity	0	+	−	−	+

Note.—+ = Merit, − = serious drawback of the strategy, 0 = neutral aspect.

† Includes preparation of phantoms and validation of the strategy.

Figure 1

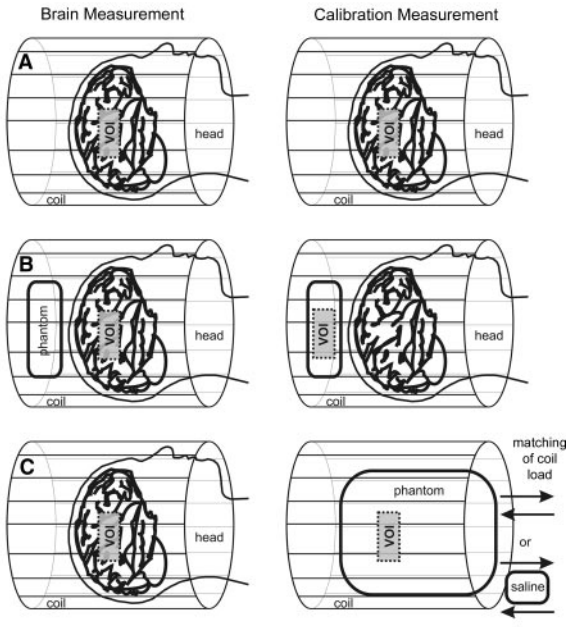

Figure 1: Schematic illustrates experimental setup of calibration strategies used for quantification of cerebral metabolite concentrations. Left: Setup for brain examination. Right: Calibration measurement. *A,* Internal endogenous marker, water signal reference method, and principle of reciprocity. *B,* External reference method. *C,* Replace-and-match method.

siderably different from that in the human head. Therefore, simple matching of the conductivity and overall load might be insufficient, because the human head has structures of varying resistance that alter electric current paths.

Water signal reference method.—Several research groups have used tissue water as an internal standard (32,45–50). The in vivo measurement is performed first. Then, from the same voxel, the signal from unsuppressed tissue water is recorded, which serves as an endogenous concentration reference (Fig 1, *A*). It is best to record the water-suppressed spectra under conditions that are identical to those for the metabolite spectra. This can be achieved by detuning or switching off the water-suppression RF pulses. The use of pure cerebrospinal fluid (recorded from a voxel that contains only cerebrospinal fluid) as a water reference to obtain molar concentrations is inadvisable, since it is usually impossible to position a voxel of sufficiently large size in an area that contains only cerebrospinal fluid (eg, ventricles).

Alternatively, the water content can be derived from proton-density–weighted images (51,52). The obtained metabolite concentrations, in molal units, can be converted into molar concentrations by using the density of brain tissue (32). Because the determination of brain density and brain water content can be quite elaborate, one usually applies a value from the literature. However, one has to be cautious since several pathologic conditions are known to affect the water content. For instance, it has been determined for conditions such as multiple sclerosis (53,54), brain tumors (55), and hydrocephalus (55) that the brain water content can be increased up to 12%, 50%, and 120%, respectively, over the water content in healthy subjects.

Principle of reciprocity.—From the principle of reciprocity (55,56), it can be deduced that (if the coil is a combined transmit-receive coil) the external voltage needed to produce a certain B_1 at a given location is inversely related to the voltage induced in the same RF coil by a predefined B_1. The calibration strategy (also referred to as the phantom-replacement strategy) that is based on this notion involves the determination of the local B_1 at the VOI, which is accomplished by measuring the voltage amplitude required to obtain the maximum signal response (V_{max}) (Fig 1, *A*). Absolute standard units can then be obtained by dividing the recorded in vivo MR signals by V_{max} and by performing additional calibration measurements with a solution of known concentration (57–61). The principle of reciprocity applies only to transmit-receive coils. For MR systems with a receive-only coil, an alternative approach based on the same principle has been designed in which the transmit-receive capabilities of the body coil are used (62).

Institutional units.—In this quantification approach, one of the previously mentioned absolute reference methods is used, but the final calibration to standard units is not performed. Therefore, this method shares the robustness of the applied AQ strategy but is only useful for diagnostic comparison within one institution.

Important Considerations for AQ

Echo time and repetition time.—When the repetition time of a pulse sequence is relatively short (generally shorter than five times the longitudinal relaxation time, T1), the magnetization cannot totally recover before the next excitation, which leads to a reduction of the signal (ie, signal saturation).

At 1.5 T, typical T1 relaxation times (± standard deviation) for several metabolites are 1430 msec ± 165 for NAA, 1330 msec ± 199 for choline, 1460 msec ± 270 for total creatine, and 1140 msec ± 308 for *myo*-inositol (32,63,64). Given these values, a repetition time of 2000 msec will lead to a decrease of the NAA signal of approximately 25%, whereas a repetition time of 7000 msec will cause a reduction of only 0.7%. Because the T1 values for most metabolites are not the same, the acquired signal intensity of each resonance should be corrected separately for partial saturation. Therefore, the use of a long repetition time is advisable since it reduces systematic errors caused by T1 signal saturation, even though this increases the duration of the MR acquisition.

Table 2

Reduction of Metabolite Peak Area as Function of Echo Time

Echo Time (msec)	NAA*	Macromolecules†
20	4.6	33.0
30	6.9	45.1
50	11.2	63.2
130	26.5	92.6
260	46.0	99.4

Note.—Data are percentage reduction in metabolite peak area with respect to hypothetic echo time of 0 msec.

* T2 relaxation time of 420 msec (32).

† T2 relaxation time of 50 msec (65).

The use of a short echo time (eg, <20 msec) minimizes signal losses caused by T2 relaxation. At 1.5 T, typical T2 relaxation times for several metabolites are 422 msec ± 48 for NAA, 356 msec ± 35 for choline, 214 msec ± 23 for total creatine, and 200 msec ± 20 for *myo*-inositol (32,51,64). The reduction of the NAA signal will be approximately 21% if an echo time of 100 msec is used, while the signal loss will only be approximately 5% if an echo time of 20 msec is used (the effect of varying echo times is indicated in Table 2). In contrast, macromolecules (compounds with a high effective molecular weight) have a very short T2 relaxation time (<50 msec at 2.1 T [65]), so the use of even the shortest echo time leads to a large reduction in signal. For instance, an echo time of 20 msec will lead to a reduction in the macromolecule signal of approximately 30%. On the other hand, spectra acquired with a long echo time (>150 msec) benefit from a less complicated appearance (mainly resonances from uncoupled spins remain visible, such as singlets from NAA, total creatine, and choline), improved water suppression, and a flatter baseline (due to signal reduction of components with short T2, such as water and macromolecules).

In all these cases, signal intensities of each resonance have to be properly corrected for T2 relaxation. However,

accurate determination of T1 and T2 is usually too time consuming to be performed for every patient (66). Unfortunately, one sometimes cannot resort to using average values of a patient group, since relaxation times may be influenced by pathologic conditions and by the severity of a specific condition. For example, for diseases such as stroke (67), amyotrophic lateral sclerosis (68), low-grade glioma, and high-grade glioma (69), the T2 relaxation times of NAA can be reduced up to 42%, 22%, 38%, and 43%, respectively.

Receiver gain instability.—In any quantification strategy that requires an additional calibration measurement of a phantom, this measurement should be recorded with exactly the same amplifier gain settings as were used for the in vivo measurement, to prevent systematic errors. Therefore, a calibration experiment is preferably performed immediately after the in vivo experiment. However, if time restrictions prevent this measurement, one has to monitor the receiver stability on a regular basis, since it is not easily corrected for afterwards. An assessment of receiver gain stability can be performed by measuring the background noise level in a region of the spectrum "downfield" from the water resonance, where no signals are expected (61). The background noise level should exhibit minimal variations if the spectrometer has good long-term stability (56).

Compartmentation.—Because in vivo MR is performed on tissue at a macroscopic level, various brain compartments (gray matter, white matter, blood, cerebrospinal fluid, or lesions) with different metabolite concentrations might contribute to the metabolite signal measured. It is hard to determine the "true" concentration level of a metabolite in a specific homogeneous tissue. For example, metabolite concentrations that are uncorrected for the contribution of cerebrospinal fluid are generally underestimated, since the concentration of ^{1}H MR spectroscopically detectable metabolites in cerebrospinal fluid is very low (70). Therefore, several tissue segmentation approaches have been proposed, all of which rely on differences in relaxation properties as determined with a separate MR imaging measurement. These methods include the use of calculated T1- or T2-weighted images (17) or spectra in which the T2 decay of water is measured as a function of echo time (50,71). However, since pathologic conditions may affect relaxation times, one should always carefully interpret results from any segmentation procedure.

MR visibility.—Not all metabolite molecules contribute equally to the MR signal from a certain VOI. For example, creatine has an invisible metabolite pool (2.5%) that is bound to macromolecular structures and, therefore, has low mobility; this results in very short T2 relaxation times and thus broad resonances, which can be unobservable on conventional MR spectra (72). A larger underestimation (up to 10% for creatine [73] and up to 30% for lactate [74]) of the true concentration can be caused by magnetization transfer effects if a water-suppression technique such as presaturation is used. However, most metabolites are not susceptible to magnetization transfer effects and show a signal change only slightly above the limits of experimental error (75). Furthermore, in most measurement methods magnetization transfer effects can generally be avoided.

Table 3

Relative Merits and Drawbacks of Data Analysis Procedures

Procedure	Preparation Time	Sensitivity to Baseline Imperfections	Ease of Use	Accuracy
Integration	+	−	+	−
Peak fitting	+	−	+	−
Peak fitting with prior knowledge	0	0	0	0
Peak fitting with metabolite basis set	−	+	−	+

Note.—+ = Merit, − = serious drawback, 0 = neutral aspect.

Data Analysis

In this section, the most important methods of data analysis will be described. The merits and drawbacks of each analysis method are shown in Table 3. The actual quantification can be performed in either the time (76) or the frequency (77) domain. In the time domain, the MR signal is represented as a function of recording time, whereas in the frequency domain the signal is represented as a function of resonance frequency. The time-dependent signal can be converted into its equivalent frequency representation by applying a Fourier transformation. In theory, there are no differences between the two domains (78), but the data are always presented in the frequency domain since this enables direct (visual) interpretation.

Integration

The traditional procedure to determine the area of a certain peak in the frequency domain is integration. The operator selects a frequency range, which preferably contains only one peak, and then performs numeric integration. Because only the total area under a resonance corresponds to the real peak intensity and the contribution beyond the lower and upper integration boundaries is neglected, the peak area will be underestimated (possibly by up to 40% [79]). Therefore, integration is an adequate method only if the resonances are well separated without any baseline fluctuations. Unfortunately, this is rarely the case, since most in vivo spectra suffer markedly from spectral overlap and baseline fluctuations. Therefore, the area can hardly be attributed to a single resonance, and, in addition, the baseline will lead to an unknown contribution.

Peak Fitting

In this approach, all important peaks are initially selected and coarse estimations of the resonance frequency, line width, and peak intensity are per-

formed, either by the operator or by an algorithm. Subsequently, a fit is performed by using a least-squares optimization algorithm, which iteratively fits all peaks to a line-shape model function, so that the fitted spectrum resembles the experimental spectrum as closely as possible (80). In general, this method proves to be fairly robust with respect to spectral overlap. However, if the actual line shapes deviate substantially from Gaussian or lorentzian model functions, the algorithm will not be able to fit the peaks accurately. To prevent this problem, other line shapes have occasionally been used, of which the Voigt profile is the most common (81). However, the use of a Voigt profile introduces more degrees of freedom in the fitting procedure, which can lead to ambiguous results.

Prior Knowledge

This method allows the incorporation of prior knowledge about the metabolites that contribute to the ^{1}H MR spectroscopic signal (82). All known signal parameters, such as relative frequencies, amplitude ratios, scalar coupling, and phases of resonances that are characteristics of a certain metabolite, can be implemented as constraints in the fitting routine. Prior knowledge is the only way of enhancing, by reducing the degrees of freedom, the accuracy of fitted model parameters for a given data set. The calculation time is also reduced. An example of a method that enables incorporation of prior knowledge is the AMARES method (Department of Electrical Engineering, Katholieke Univesiteit Leuven, Leuven, Belgium) (83).

Advanced prior knowledge obtained through metabolite basis set.—A decade ago, algorithms were proposed (82,84) that implemented a strategy where the maximum of prior knowledge is used. Those methods were based on the assumption that there are a limited number of ^{1}H MR spectroscopically detectable metabolites present in the human brain that had already been identified and analyzed in earlier studies. The approach aimed to individually determine the exact response of all metabolites possibly present to a specific pulse sequence. One has to take into account the type of imager, B_0, pulse sequence, echo time, and repetition time, as well as the pH, ion composition, and temperature of the solution in which the individual metabolites are dissolved. In this way, the prior knowledge of each metabolite—including chemical shifts, signal intensity (influenced by relaxation effects), amplitude ratios, splitting patterns, and J evolution—matches the in vivo conditions. The in vivo MR spectra are then analyzed as a linear combination of the separately recorded in vitro spectra of the individual metabolites.

There are two commonly used approaches for obtaining a basis set: simulation and in vitro measurement. In the simulation approach (85,86), the response is numerically simulated on the basis of molecular and quantum mechanical characteristics of each metabolite (87,88). The in vitro approach (89) requires that for each metabolite, a spectrum is acquired with exactly the same conditions (eg, pulse sequence and timing parameters) as those used during the in vivo measurements. The advantage of the simulation approach is that, as long as the exact molecular structure is known, each metabolite can be included, whereas the in vitro approach requires carefully prepared metabolite phantoms. The advantage of the in vitro approach is that, as long as the phantoms are adequately prepared, the response of the metabolites in the in vitro measurement will be identical to the response of the metabolites in the in vivo ^{1}H MR spectroscopy examination.

The high information content of ^{1}H MR spectra leads to an advantage regarding the fitting accuracy, because overlapping resonances at one chemical shift position can be directly related to other nonoverlapping resonances from the same metabolite. Currently used computer software includes the metabolite basis set fitting program LCModel (Stephen Provender, PhD, *http://s-provender.com/pages/lcmodel.shtml*) (84), possibly incorporating the molecular simulation library GAMMA (Department of Radiology, University of California, San Francisco) (87); the quantification package jMRUI (The MRUI Project, *http://sermn02.uab.es/mrui/*) (90), which includes the quantum mechanical simulation algorithm NMR-SCOPE (Laboratoire de RMN, Universite Lyon I-CPE, Villeurbanne, France) (88); and the metabolite basis set fitting routine QUEST (Laboratoire de RMN, Universite Lyon I-CPE) (85) and the algorithm TDFDFit (Department of MR Spectroscopy and Methodology, University and Inselspital, Berne, Switzerland) (91). A detailed description (92) and a critical assessment (7) of both AMARES and LCModel can be found elsewhere. Examples of LCModel output and TDFDfit output are given in Figures 2 and 3, respectively.

One should note that the T1 and/or T2 relaxation times are not always the same in the in vitro and the in vivo situations, and different resonances in the same metabolite might have different relaxation times. For example, the methylene protons of creatine, $^{2}CH_2$, which resonate at around 3.90 ppm, display shorter T1 and T2 relaxation times (31% for T1 and 28% for T2, measured at 3 T) than do the methyl protons of creatine, $N(CH_3)$, which resonate at around 3.03 ppm (93). Therefore, in pathologic conditions that are known to affect relaxation times, in vitro prior knowledge cannot always be applied to in vivo ^{1}H MR spectra, which may lead to systematic errors (see previous discussion on echo time and repetition time in Important Considerations for AQ). In that case, a separate relaxation measurement would be favorable.

Important Considerations for Data Analysis

Quantification accuracy.—It is important to study and report the error estimates of the quantification method. Most of the fitting routines present the so-called Cramer-Rao minimum variance bounds (CRMVBs), which reflect the theoretic standard of precision for the model parameter estimates obtained from the data (94). The parameter estimation must not contain systematic errors (eg, incorrect prior knowledge), which may lead to underestimation errors. It is important to realize that the CRMVBs provide a measure of quality of the spectral fit and do not necessarily reflect the quality of the

original data. Furthermore, SNR degradation and increases in line width, which may lead to systematic errors, are not necessarily reflected in CRMVB estimates (95).

Macromolecules

Macromolecules are compounds with a relatively high molecular weight and include proteins and polypeptides. Owing to their lower mobility, macromolecules generally have a short T2 and are thus characterized by broad spectral lines on [1]H MR spectra. Macromolecules are the main contributors to the fluctuating baseline that generally hinders accurate quantification of small metabolites. Some macromolecular resonances even overlap completely with sharp metabolite resonances and, therefore, cannot even be accounted for with conventional [1]H MR spectroscopy (65,96). Several methods can be used to separate the macromolecular baseline from the wanted metabolite signal.

The best way to eliminate macromolecular contamination is to use acquisition schemes that exploit the different relaxation properties of macromolecules and small metabolites. Removal based on T1 relaxation can be achieved by so-called inversion-recovery (65) or saturation-recovery (97) sequences (Fig 4), whereas removal based on T2 relaxation can be obtained by increasing the echo time (32).

Figure 2

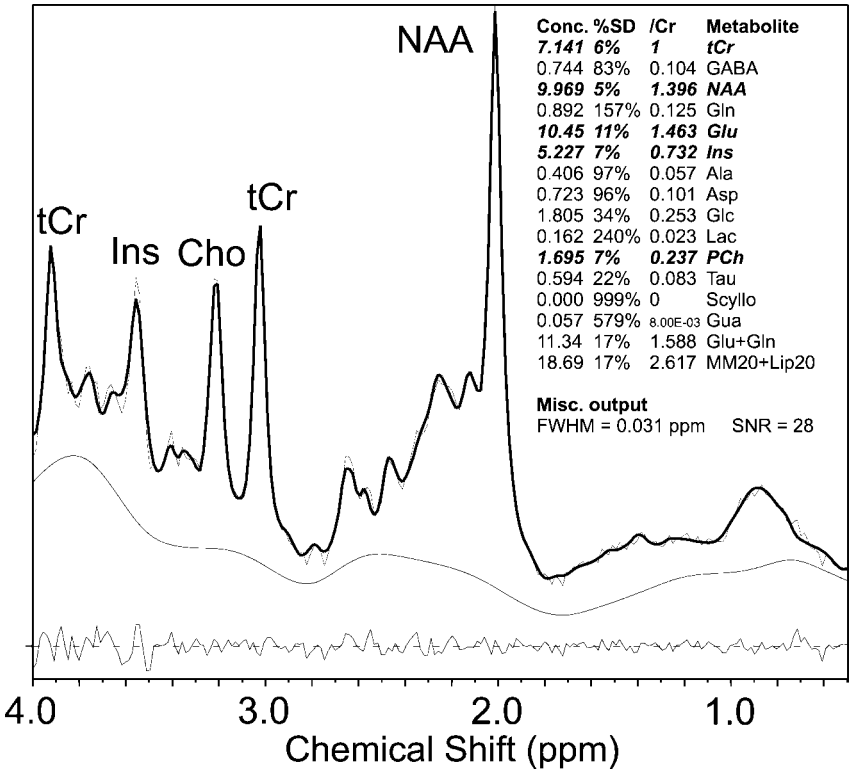

Figure 2: [1]H MR spectrum analyzed with LCModel (version 6.1-4) output of point-resolved spatially localized spectroscopy in a healthy adult subject. Spectra were recorded at 1.5 T (Intera; Philips Medical Systems, Best, the Netherlands) from the occipital lobe (repetition time msec/echo time msec, 2000/23; 128 signals acquired; voxel size, 8 cm^3). In vivo spectrum (thin upper spectrum) was estimated with LCModel output (thick upper spectrum); the difference between spectra is plotted at the bottom. Above the difference spectrum is the baseline spline estimate, determined with LCModel. Inserted table at right displays estimated metabolite concentrations and Cramer-Rao minimum variance bounds. *Cho* = choline, *Conc.* = concentration, *Cr* = creatine, *FWHM* = full width at half maximum, *Ins* = *myo*-inositol, *SD* = standard deviation, *tCr* = total creatine.

Alternatively, a pure metabolite spectrum can be obtained by subtracting a macromolecules spectrum (similarly obtained by exploiting the relaxation differences) from the acquired in vivo spectrum (98). Unfortunately, in vivo determination of the exact relaxation times for both macromolecules and metabolites is complicated and time consuming. Furthermore, neither metabolites nor macromolecules necessarily display a narrow distribution of relaxation times, which means that removal based on relaxation times will not always yield good results. During postprocessing, the macromolecular signal can be estimated by using a spline or polynomial function, which can be subtracted from the original spectrum to improve the baseline (84). However, since this approach relies on an estimation, it is not flawless.

Recently, it has become popular to include the macromolecules baseline in the fitting routine (20,89,99). With the LCModel approach, it is possible to extend the metabolite basis set with a macromolecules spectrum. Since the macromolecular contribution to in vivo spectra cannot be simulated with simple model solutions, one has to determine the macromolecules baseline experimentally. Both inversion recovery (89) and saturation recovery (100) have been used to obtain macromolecules baseline spectra, which were averaged over several subjects and then parameterized to be included in the basis set. The incorporation of macromolecules into the basis set generally improves quantification accuracy and precision (101).

Macromolecules themselves have been the subject of recent research (65,102). It has been reported that several conditions, such as stroke (103), brain tumors (101), and multiple sclerosis (99), show an altered macromolecular profile. For example, stroke (103) and multiple sclerosis (99), respectively, can cause the signal occurring from the macromolecules resonance at 1.3 ppm to increase by 86% and 60%. Therefore, one should always carefully consider the incorporation of macromolecules spectra in

the basis set when such a condition is of concern.

Motion

Physiologic motion can have a large effect on [1]H MR spectroscopic quantification (104). For example, repeated small body motions or pulsatile cerebral motion (eg, due to cardiac activity), can substantially affect the characteristics of the MR signal, even with motion-compensated [1]H MR spectroscopy sequences. These effects may include an increase in line width, reduced peak intensities, a diminished quality of water suppression, or a doubling of all peaks. Moreover, if quantification is based on the summed signal of reference spectra of the unsuppressed water peak, motion-induced phase effects can cause a substantial overestimation of metabolite concentrations, a problem that can be circumvented by storing and phasing all spectra individually (104). For chemical shift imaging studies that include subcutaneous lipid signals, which have an enhanced sensitivity to subject motion, an in-plane motion correction can be applied (105). The reduction of motion effects in [1]H MR spectroscopy has been achieved in several studies (eg, by using cardiac triggering [104] or postprocessing [106]).

VOI Shape and Location

In the process of spectral quantification, one should always keep in mind that the true spatial voxel profile might deviate from a perfect rectangular profile. The voxel dimensions are, in principle, identical for all resonances; however, the voxel position is dependent on the chemical shift of individual resonances. When a section-selective gradient is applied to a volume containing metabolites with different chemical shifts, there will be a displacement of the sensitive volume for each resonance of the metabolite. The displacement is regulated by the bandwidth of the RF pulse for voxel selection (38). For example, the methyl protons of NAA and the methylene protons of total creatine are separated by 1.90 ppm, or 122 Hz, at 1.5 T. Use of an RF bandwidth of 2000 Hz and a voxel size of 2 × 2 × 2 cm results in a 1.22-mm displacement of the 2 voxels, which results in an 82.8% overlap of the 2 voxels.

Chemical shift artifacts can be reduced by increasing the bandwidth of the section-selective RF pulses and, to keep the same voxel dimensions, by increasing the strength of section-selective gradients. Obviously, safety margins should not be exceeded. It should be noted that chemical shift imaging does not suffer from the chemical shift artifact for the spatial phase-encoding gradients, which are applied in the ab-

Figure 3

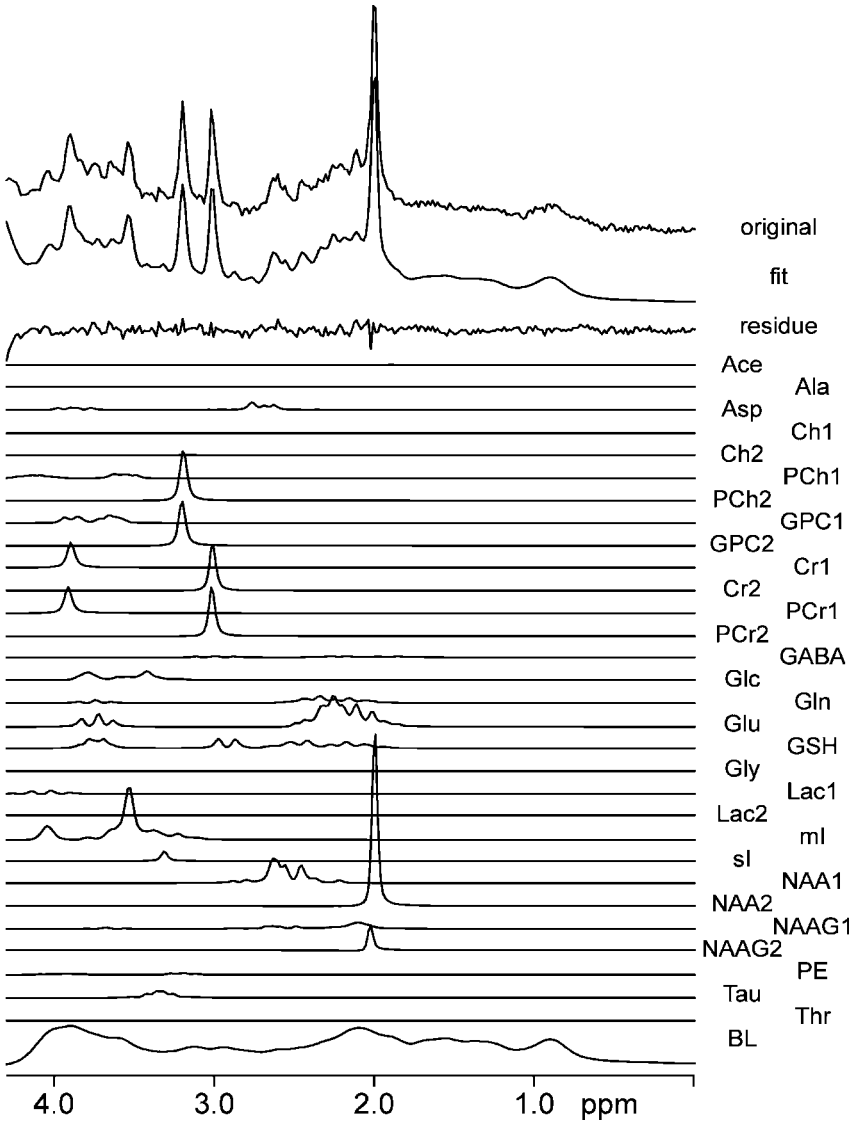

Figure 3: Fit results for point-resolved spatially localized [1]H MR spectrum (3000/20; 128 signals acquired; voxel size, 16 cm^3) obtained at 1.5 T (Signa; GE Healthcare, Milwaukee, Wis) from white matter in centrum semiovale of an 18-year-old control subject. Parameterized fitting with metabolite basis set fitting algorithm TDFDfit was used. At top are experimental spectrum, fitted spectrum, and residuals. Below are traces for the individual components that add up to the best fit (see reference 100 for definition of abbreviations). Some metabolites were split into two spectra, providing the freedom of differential T2 values for different protons in the same molecule. Baseline spectrum was obtained from a saturation recovery experiment. (Reprinted, with permission, from reference 100.)

sence of RF pulses. However, if the chemical shift imaging study involves preselection of a VOI (eg, to exclude skull lipids) then the position of that VOI is again subject to the chemical shift artifact, while the chemical shift imaging voxels within the VOI are not shifted with respect to each other. Chemical shift imaging data are also influenced by the point-spread function, which will be treated in the section entitled Sequence-Specific Issues.

Line Shape and Eddy Currents

Very often, the line shape of signals obtained from metabolites deviates substantially from the ideal lorentzian line shape. If left uncorrected, these line shape deviations severely complicate peak fitting. Generally, line shape deviations are caused by variations in B_0, such as magnetic field inhomogeneities and eddy currents. Rapid switching of magnetic field gradients (which occurs in every localization pulse sequence) induces time-varying eddy currents in the magnetic cryostat. As a result, the magnetic field is transiently distorted. Several methods have been developed to correct irregular line shapes, including the QUALITY deconvolution (107) and eddy current correction procedure (108). These correction methods use a single reference peak that was affected by the same distortions. The unsuppressed water signal, acquired by using the same spoiler gradients as the metabolite spectrum, is usually used for that purpose.

Figure 4

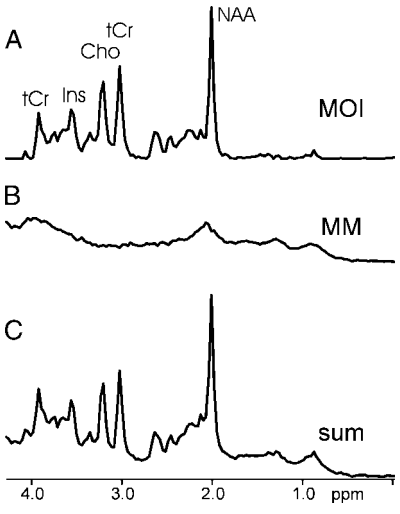

Figure 4: Point-resolved spatially localized ^{1}H MR spectra obtained at 1.5 T (Signa, GE Healthcare) in a healthy adult. Spectra (6000/20; 128 signals acquired; voxel size, 12 cm^3) were recorded from the centrum semiovale. *A,* Metabolites-of-interest *(MOI)* spectrum. B, Macromolecules-only *(MM)* spectrum. *C,* Sum spectra calculated from series of saturation-recovery spectra. *Cho* = choline, *Ins* = *myo*-inositol, *tCr* = total creatine. (Reprinted, with permission, from reference 97.)

Water Suppression

As indicated earlier, water-suppression pulses might saturate parts of the metabolite spectrum and can thus influence the measured concentration of several metabolites (a reduction of up to 21% has been reported [109]). Numeric calculations can be employed for accurate corrections for these effects (109). In addition, the residual water signal that is still present in water-suppressed spectra can substantially degrade the performance of metabolite fitting routines. Therefore, it is advisable to eliminate the unwanted water signal by using a high-pass filter (110) or an algorithm such as the Hankel-Lanczos singular-values decomposition filter (111) prior to data analysis (Fig 5).

Figure 5

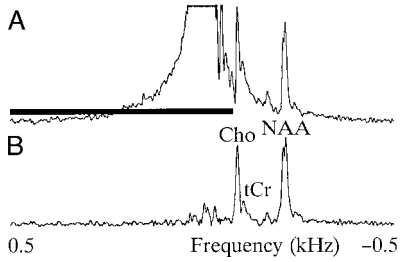

Figure 5: Water signal removal by means of Hankel-Lanczos singular-values decomposition filter. In vivo chemical shift imaging ^{1}H MR spectroscopy in the brain of a healthy adult. *A,* Region indicated by horizontal bar contains the water peak. The peaks of interest, choline *(Cho),* total creatine *(tCr),* and NAA, are disturbed by right tail of the water peak. *B,* Spectrum after subtraction of water signal components, as retrieved and quantified with the Hankel-Lanczos singular-values decomposition filter in region of the horizontal bar in *A.* Components outside horizontal bar region are not affected by the procedure. (Reprinted, with permission, from reference 111.)

Sequence-Specific Issues

Spectral Editing

Lately, several clinical studies have been performed using the spectral editing approach (112,113). Spectral editing enables detection of metabolites that are hard to detect with conventional ^{1}H MR spectroscopic techniques because these metabolites are present in lower concentrations and their resonance peaks overlap with those of other more abundant metabolites (114). By using a specifically designed acquisition scheme that allows selective recording of signals only from desired metabolite(s), the information content of the acquired signal is reduced. Preferably, only peaks of the desired metabolite(s) remain in the spectrum, while the other metabolites are eliminated. Among the metabolites that are the target of the spectral editing approach are γ-aminobutyric acid, glutamine, lactate, and glutathione.

It is important that the pulse sequence be carefully optimized and that the specificity of the editing procedure be critically assessed. If unwanted signals remain in the final spectrum, simple peak fitting will not suffice, although one could resort to the advanced prior knowledge approach (115).

Chemical Shift Imaging

Quantification of chemical shift imaging data generally requires extra considerations, because chemical shift imaging data can be different from single-voxel data in some respects. For example, chemical shift imaging data usually have a lower SNR, since these imaging data are subject to field inhomogeneities (due to the large VOI). In addition, chemical shift imaging data are also subject to artifacts such as imperfect water-suppression and lipid-contamination artifacts. On the other hand, the spatial information of chemical shift imaging offers several opportunities to improve postprocessing and analysis. Knowl-

edge of the spatial dependence of parameters may yield extra information with regard to prior knowledge or constraints. For instance, the notion that voxel-to-voxel variations in metabolite concentrations can be expected to change smoothly can be used to set constraints on the limits of these variations (116).

Not all AQ strategies are necessarily compatible with chemical shift imaging data. For example, it is often too time consuming to obtain fully relaxed water reference spectra with the same resolution (117). A commonly used referencing scheme for chemical shift imaging is the time-efficient reciprocity principle (21,61). An absolute reference can also be obtained by means of proton-density–weighted MR imaging (40).

Point-spread function.—Quantification of chemical shift imaging data is complicated by the point-spread function, which describes the spread of signal from one voxel to surrounding voxels. The point-spread function originates from Fourier transformation of a signal sampled in the time domain at a limited number of discrete points. Although the point-spread function influences all Fourier-transformed data, in chemical shift imaging the effect may become prominent since chemical shift imaging data are generally acquired with a relatively low spatial resolution, corresponding to a small number of phase-encoding increments.

The point-spread function, and therefore the spatial resolution, can be improved by applying apodization functions in the spatial frequency or k-space domain (118). One approach is to apply different k-space sampling schemes to improve the point-spread function and the SNR (119,120). Another approach is k-space weighting during signal acquisition, which also yields a better SNR (121). In chemical shift imaging of the brain, the point-spread function effect will typically lead to contamination of ^{1}H MR spectra of voxels within the brain by intense extracranial lipid signals. k-Space weighting or application of apodization functions to improve the point-spread function is usually insufficient in this case; therefore, other methods, such as outer volume suppression, are used to prevent lipid signals from contaminating brain spectra.

Other methods reduce lipid contamination during postacquisition processing (122). In an AQ strategy, coregistered MR images are generally used for tissue segmentation (T1- or T2-weighted MR imaging [17]) or for water referencing (proton-density–weighted MR imaging [40,52]). It is important to note that apodization filters, used to improve the point-spread function of the metabolite spectra, should also be applied to the MR imaging data that are used for the segmentation procedure.

Fully automated spectral analysis.—Analysis of spectra from large chemical shift imaging data sets is time consuming, and because usually only spectra from a few selected voxels are analyzed, the complete data set is often underutilized. Therefore, automated methods have been developed (87,116,117) that enable analysis of large numbers of spectra and that are relatively insensitive to the low SNR and spectral distortions commonly associated with in vivo chemical shift imaging. Furthermore, the introduction of a standardized processing and analysis protocol makes comparisons between different studies possible.

Quality Assessment

Generally speaking, spectra with a large line width, low SNR, or obvious artifacts (ie, signal contributions from outside the VOI, phase distortions, and technical failures) should be discarded. In addition, when studying certain pathologic conditions, it is important to establish the limits of metabolite concentrations that represent abnormality. To obtain reliable absolute concentrations for the assessment of pathologic changes, it is necessary to take both the data acquisition methods and the data processing methods into account. Overall reproducibility depends on the variability at immediate repetition of an acquisition, intraindividual variability at reexamination of the same subject at a subsequent acquisition, and interindividual variability. The achievable overall reproducibility values for the AQ of NAA, total creatine, choline, and *myo*-inositol have been published for single-voxel spectroscopy and range from 7% to 16% (27,100); for chemical shift imaging, reproducibility values range from 5% to 21% (123,124). Therefore, to detect an abnormality, the deviation from normal values should be larger than the reproducibility of that particular measurement.

SNR Considerations

The SNR can be used as a measure in the rejection of spectra (eg, the SNR should generally be at least 4). The SNR is usually defined in the frequency domain as the ratio of the highest metabolite peak intensity to the standard deviation of the noise amplitude in a metabolite-free part of the spectrum (118). The SNR can be improved by increasing the size of the VOI and the number of signal averages acquired. However, an increase in the size of the VOI generally degrades the line shape, increases the line width, and may decrease the sensitivity to detect abnormalities, whereas an increase in the number of signals acquired adds to the examination time.

Line Width

The line width is commonly defined as the full width of the peak at half its maximum height, or full width at half maximum, in the frequency domain (118). A small line width generally implies a high spectral resolution, which will improve the quality of the fitting routines. Better shimming, the use of a smaller VOI, and the choice of a VOI at a sufficient distance from tissue interfaces can improve the resolution. It has been recommended that the full width at half maximum value should always be treated as a covariate in the statistical analysis, to help correct for single-subject intersession variations (27).

Criteria for Rejection of Data

In a recent insightful review, Kreis (125) proposed the following acceptance criteria for spectral data and their fitting results: *(a)* The full width at half maximum of the metabolites should be less than 0.1 ppm; *(b)* the Cramer-Rao

minimum variance bound should be smaller than 50%; *(c)* the fitting residual should not contain unexplained features; and *(d)* the spectra should not contain artifacts (eg, doubled peaks or asymmetric line shapes).

Conclusions and Future Perspectives

The implementation of AQ in a clinical routine has been greatly facilitated by the development of calibration strategies and the availability of spectral fitting routines. This is beneficial progress because AQ has an added value for ^{1}H MR spectroscopic quantification. Furthermore, the introduction of phased-array coils (126) and higher (>1.5-T) field strengths (127) has been proved to be advantageous with regard to SNR, quantification precision, reproducibility, and detection sensitivity. To obtain reliable absolute concentrations, however, one has to consider potential complicating factors, with respect to both the data acquisition method and the data processing method. For example, relaxation effects in data acquisition can be either corrected for or eliminated, whereas data fitting is complicated by factors such as contribution of macromolecules. Nevertheless, most of these problems have been critically addressed and can be taken into account in a satisfying manner. AQ is available and can improve the diagnostic utility of ^{1}H MR spectroscopy procedures. Therefore, further progress in the development of automated spectral analysis methods and databases of normal regional and age-dependent metabolite concentrations has to be encouraged to make the AQ procedures more easily applicable in clinical routine.

References

1. Ross B, Bluml S. Magnetic resonance spectroscopy of the human brain. Anat Rec 2001;265:54–84.
2. Alger JR, Cloughesy TF. Structural and functional imaging of cerebral neoplasia. In: Mazziotta JC, Toga AW, Frackowiak RSJ, eds. Brain mapping: the disorders. San Diego, Calif: Academic Press, 2000.
3. Chu WC, Chik KW, Chan YL, et al. White matter and cerebral metabolite changes in children undergoing treatment for acute lymphoblastic leukemia: longitudinal study with MR imaging and 1H MR spectroscopy. Radiology 2003;229:659–669.
4. Vermathen P, Laxer KD, Schuff N, Matson GB, Weiner MW. Evidence of neuronal injury outside the medial temporal lobe in temporal lobe epilepsy: N-acetylaspartate concentration reductions detected with multisection proton MR spectroscopic imaging—initial experience. Radiology 2003; 226:195–202.
5. Rai GS, McConnell JR, Waldman A, Grant D, Chaudry M. Brain proton spectroscopy in dementia: an aid to clinical diagnosis. Lancet 1999;353:1063–1064.
6. Ruiz-Pena JL, Pinero P, Sellers G, et al. Magnetic resonance spectroscopy of normal appearing white matter in early relapsing-remitting multiple sclerosis: correlations between disability and spectroscopy. BMC Neurol 2004;4:8.
7. Kanowski M, Kaufmann J, Braun J, Bernarding J, Tempelmann C. Quantitation of simulated short echo time 1H human brain spectra by LCModel and AMARES. Magn Reson Med 2004;51:904–912.
8. Kreis R. Quantitative localized (1)H MR spectroscopy for clinical use. J Prog NMR 1997;31:155–195.
9. Cady E. Determination of absolute concentrations of metabolites from NMR spectra. NMR Basic Princ Prog 1992;26:249–281.
10. Henriksen O. In vivo quantitation of metabolite concentrations in the brain by means of proton MRS. NMR Biomed 1995;8:139–148.
11. Tofts PS, Wray S. A critical assessment of methods of measuring metabolite concentrations by NMR spectroscopy. NMR Biomed 1988;1:1–10.
12. Stoppe G, Bruhn H, Pouwels PJ, Hanicke W, Frahm J. Alzheimer disease: absolute quantification of cerebral metabolites in vivo using localized proton magnetic resonance spectroscopy. Alzheimer Dis Assoc Disord 2000;14:112–119.
13. Mueller SG, Laxer KD, Suhy J, Lopez RC, Flenniken DL, Weiner MW. Spectroscopic metabolic abnormalities in mTLE with and without MRI evidence for mesial temporal sclerosis using hippocampal short-TE MRSI. Epilepsia 2003;44:977–980.
14. Savic I, Osterman Y, Helms G. MRS shows syndrome differentiated metabolite changes in human-generalized epilepsies. Neuroimage 2004;21:163–172.
15. Simister RJ, Woermann FG, McLean MA, Bartlett PA, Barker GJ, Duncan JS. A short-echo-time proton magnetic resonance spectroscopic imaging study of temporal lobe epilepsy. Epilepsia 2002;43: 1021–1031.
16. Fernando KT, McLean MA, Chard DT, et al. Elevated white matter myo-inositol in clinically isolated syndromes suggestive of multiple sclerosis. Brain 2004;127:1361–1369.
17. Hetherington HP, Pan JW, Mason GF, et al. Quantitative 1H spectroscopic imaging of human brain at 4.1 T using image segmentation. Magn Reson Med 1996;36:21–29.
18. Auer DP, Schirmer T, Heidenreich JO, Herzog J, Putz B, Dichgans M. Altered white and gray matter metabolism in CADASIL: a proton MR spectroscopy and 1H-MRSI study. Neurology 2001;56:635–642.
19. Pohl C, Block W, Karitzky J, et al. Proton magnetic resonance spectroscopy of the motor cortex in 70 patients with amyotrophic lateral sclerosis. Arch Neurol 2001;58: 729–735.
20. Auer DP, Gossl C, Schirmer T, Czisch M. Improved analysis of 1H-MR spectra in the presence of mobile lipids. Magn Reson Med 2001;46:615–618.
21. McLean MA, Woermann FG, Barker GJ, Duncan JS. Quantitative analysis of short echo time (1)H-MRSI of cerebral gray and white matter. Magn Reson Med 2000;44: 401–411.
22. Connelly A, Jackson GD, Duncan JS, King MD, Gadian DG. Magnetic resonance spectroscopy in temporal lobe epilepsy. Neurology 1994;44:1411–1417.
23. Lundbom N, Gaily E, Vuori K, et al. Proton spectroscopic imaging shows abnormalities in glial and neuronal cell pools in frontal lobe epilepsy. Epilepsia 2001;42:1507–1514.
24. Mathews VP, Barker PB, Blackband SJ, Chatham JC, Bryan RN. Cerebral metabolites in patients with acute and subacute strokes: concentrations determined by quantitative proton MR spectroscopy. AJR Am J Roentgenol 1995;165:633–638.
25. Chang L, Ernst T, Tornatore C, et al. Metabolite abnormalities in progressive multifocal leukoencephalopathy by proton magnetic resonance spectroscopy. Neurology 1997;48:836–845.
26. Li BS, Wang H, Gonen O. Metabolite ratios to assumed stable creatine level may confound the quantification of proton brain MR spectroscopy. Magn Reson Imaging 2003; 21:923–928.

27. Schirmer T, Auer DP. On the reliability of quantitative clinical magnetic resonance spectroscopy of the human brain. NMR Biomed 2000;13:28–36.

28. Bottomley PA, inventor; General Electric, assignee. Selective volume method for performing localized NMR spectroscopy. U.S. patent 4,480,228 0ctober 30, 1984.

29. Frahm J, Merboldt KD, Hanicke W. Localized proton spectroscopy using stimulated echoes. J Magn Reson 1987;72:502–508.

30. Brown TR, Kincaid BM, Ugurbil K. NMR chemical shift imaging in three dimensions. Proc Natl Acad Sci U S A 1982;79:3523–3526.

31. Maudsley AA, Hilal SK, Perman WH, Simon HE. Spatially resolved high resolution spectroscopy by "four-dimensional" NMR. J Magn Reson 1983;51:147–152.

32. Kreis R, Ernst T, Ross BD. Absolute quantitation of water and metabolites in the human brain. II. Metabolite concentrations. J Magn Reson B 1993;102:9–19.

33. Fatouros PP, Heath DL, Beaumont A, et al. Comparison of NAA measures by MRS and HPLC. Acta Neurochir Suppl 2000;76:35–37.

34. Huppi PS, Fusch C, Boesch C, et al. Regional metabolic assessment of human brain during development by proton magnetic resonance spectroscopy in vivo and by high-performance liquid chromatography/gas chromatography in autopsy tissue. Pediatr Res 1995;37:145–150.

35. Bottomley PA, Weiss RG. Noninvasive localized MR quantification of creatine kinase metabolites in normal and infarcted canine myocardium. Radiology 2001;219:411–418.

36. Battistuta J, Bjartmar C, Trapp BD. Postmortem degradation of N-acetyl aspartate and N-acetyl aspartylglutamate: an HPLC analysis of different rat CNS regions. Neurochem Res 2001;26:695–702.

37. Burri R, Bigler P, Straehl P, Posse S, Colombo JP, Herschkowitz N. Brain development: 1H magnetic resonance spectroscopy of rat brain extracts compared with chromatographic methods. Neurochem Res 1990;15:1009–1016.

38. de Graaf RA, Rothman D. In vivo detection and quantification of scalar coupled (1)H NMR resonances. Concepts Magn Reson 2001;13:32–76.

39. Roth K, Hubesch B, Meyerhoff DJ, et al. Noninvasive quantitation of phosphorus metabolites in human-tissue by NMR-spectroscopy. J Magn Reson 1989;81:299–311.

40. Alger JR, Symko SC, Bizzi A, Posse S, DesPres DJ, Armstrong MR. Absolute quantitation of short TE brain 1H-MR spectra and spectroscopic imaging data. J Comput Assist Tomogr 1993;17:191–199.

41. Webb P, Spielman D, Macovski A. Inhomogeneity correction for in vivo spectroscopy by high-resolution water referencing. Magn Reson Med 1992;23:1–11.

42. Li S, Williams GD, Frisk TA, Arnold BW, Smith MB. A computer simulation of the static magnetic field distribution in the human head. Magn Reson Med 1995;34:268–275.

43. Buchli R, Boesiger P. Comparison of methods for the determination of absolute metabolite concentrations in human muscles by 31P MRS. Magn Reson Med 1993;30:552–558.

44. Duc CO, Weber OM, Trabesinger AH, Meier D, Boesiger P. Quantitative 1H MRS of the human brain in vivo based on the stimulation phantom calibration strategy. Magn Reson Med 1998;39:491–496.

45. Christiansen P, Henriksen O, Stubgaard M, Gideon P, Larsson HB. In vivo quantification of brain metabolites by 1H-MRS using water as an internal standard. Magn Reson Imaging 1993;11:107–118.

46. Danielsen ER, Henriksen O. Absolute quantitative proton NMR spectroscopy based on the amplitude of the local water suppression pulse: quantification of brain water and metabolites. NMR Biomed 1994;7:311–318.

47. Knight-Scott J, Haley AP, Rossmiller SR, et al. Molality as a unit of measure for expressing 1H MRS brain metabolite concentrations in vivo. Magn Reson Imaging 2003;21:787–797.

48. Thulborn KT, Ackerman JH. Absolute molar concentrations by NMR in inhomogeneous B1: a scheme for analysis of in vivo metabolites. J Magn Reson 1983;55:357–371.

49. Barker PB, Soher BJ, Blackband SJ, Chatham JC, Mathews VP, Bryan RN. Quantitation of proton NMR spectra of the human brain using tissue water as an internal concentration reference. NMR Biomed 1993;6:89–94.

50. Ernst T, Kreis R, Ross BD. Absolute quantitation of water and metabolites in the human brain. I. Compartments and water. J Magn Reson B 1993;102:1–8.

51. Brooks JC, Roberts N, Kemp GJ, Martin PA, Whitehouse GH. Magnetic resonance imaging-based compartmentation and its application to measuring metabolite concentrations in the frontal lobe. Magn Reson Med 1999;41:883–888.

52. Schuff N, Ezekiel F, Gamst AC, et al. Region and tissue differences of metabolites in normally aged brain using multislice 1H magnetic resonance spectroscopic imaging. Magn Reson Med 2001;45:899–907.

53. Laule C, Vavasour IM, Moore GR, et al. Water content and myelin water fraction in multiple sclerosis: a T2 relaxation study. J Neurol 2004;251:284–293.

54. Helms G. Volume correction for edema in single-volume proton MR spectroscopy of contrast-enhancing multiple sclerosis lesions. Magn Reson Med 2001;46:256–263.

55. Grasso G, Alafaci C, Passalacqua M, et al. Assessment of human brain water content by cerebral bioelectrical impedance analysis: a new technique and its application to cerebral pathological conditions. Neurosurgery 2002;50:1064–1072.

56. Hoult DI, Richards RE. The signal-to-noise ratio of the nuclear magnetic resonance experiment. J Magn Reson 1976;24:71–85.

57. Helms G. A precise and user-independent quantification technique for regional comparison of single volume proton MR spectroscopy of the human brain. NMR Biomed 2000;13:398–406.

58. Kreis R, Slotboom J, Pietz J, Jung B, Boesch C. Quantitation of localized (31)P magnetic resonance spectra based on the reciprocity principle. J Magn Reson 2001;149:245–250.

59. Kreis R, Hofmann L, Kuhlmann B, Boesch C, Bossi E, Huppi PS. Brain metabolite composition during early human brain development as measured by quantitative in vivo 1H magnetic resonance spectroscopy. Magn Reson Med 2002;48:949–958.

60. Michaelis T, Merboldt KD, Bruhn H, Hanicke W, Frahm J. Absolute concentrations of metabolites in the adult human brain in vivo: quantification of localized proton MR spectra. Radiology 1993;187:219–227.

61. Soher BJ, van Zijl PC, Duyn JH, Barker PB. Quantitative proton MR spectroscopic imaging of the human brain. Magn Reson Med 1996;35:356–363.

62. Jost G, Harting I, Heiland S. Quantitative single-voxel spectroscopy: the reciprocity principle for receive-only head coils. J Magn Reson Imaging 2005;21:66–71.

63. Ethofer T, Mader I, Seeger U, et al. Comparison of longitudinal metabolite relaxation times in different regions of the human brain at 1.5 and 3 tesla. Magn Reson Med 2003;50:1296–1301.

64. Rutgers DR, Kingsley PB, van der Grond J. Saturation-corrected T 1 and T 2 relaxation times of choline, creatine and N-acetyl aspartate in human cerebral white matter at 1.5 T. NMR Biomed 2003;16:286–288.

65. Behar KL, Rothman DL, Spencer DD, Petroff OA. Analysis of macromolecule resonances in 1H NMR spectra of human brain. Magn Reson Med 1994;32:294–302.

66. Kreis R, Slotboom J, Hofmann L, Boesch C. Integrated data acquisition and processing to determine metabolite contents, relaxation times, and macromolecule baseline in single examinations of individual subjects. Magn Reson Med 2005;54:761–768.

67. Walker PM, Ben Salem D, Lalande A, Giroud M, Brunotte F. Time course of NAA T2 and ADC(w) in ischaemic stroke patients: 1H MRS imaging and diffusion-weighted MRI. J Neurol Sci 2004;220:23–28.

68. Hanstock CC, Cwik VA, Martin WR. Reduction in metabolite transverse relaxation times in amyotrophic lateral sclerosis. J Neurol Sci 2002;198:37–41.

69. Isobe T, Matsumura A, Anno I, et al. Quantification of cerebral metabolites in glioma patients with proton MR spectroscopy using T2 relaxation time correction. Magn Reson Imaging 2002;20:343–349.

70. Lynch J, Peeling J, Auty A, Sutherland GR. Nuclear magnetic resonance study of cerebrospinal fluid from patients with multiple sclerosis. Can J Neurol Sci 1993;20:194–198.

71. Helms G. T2-based segmentation of periventricular paragraph sign volumes for quantification of proton magnetic paragraph sign resonance spectra of multiple sclerosis lesions. MAGMA 2003;16:10–16.

72. Kruiskamp MJ, de Graaf RA, van Vliet G, Nicolay K. Magnetic coupling of creatine/phosphocreatine protons in rat skeletal muscle, as studied by (1)H-magnetization transfer MRS. Magn Reson Med 1999;42:665–672.

73. Kruiskamp MJ, de Graaf RA, van der Grond J, Lamerichs R, Nicolay K. Magnetic coupling between water and creatine protons in human brain and skeletal muscle, as measured using inversion transfer (1)H-MRS. NMR Biomed 2001;14:1–4.

74. Kotitschke K, Schnackerz KD, Dringen R, Bogdahn U, Haase A, von Kienlin M. Investigation of the 1H NMR visibility of lactate in different rat and human brain cells. NMR Biomed 1994;7:349–355.

75. Leibfritz D, Dreher W. Magnetization transfer MRS. NMR Biomed 2001;14:65–76.

76. Vanhamme L, Sundin T, Hecke PV, Huffel SV. MR spectroscopy quantitation: a review of time-domain methods. NMR Biomed 2001;14:233–246.

77. Mierisova S, Ala-Korpela M. MR spectroscopy quantitation: a review of frequency domain methods. NMR Biomed 2001;14:247–259.

78. Abildgaard F, Gesmar H, Led JJ. Quantitative-analysis of complicated nonideal Fourier-transform NMR-spectra. J Magn Reson 1988;79:78–89.

79. Meyer RA, Fisher MJ, Nelson SJ, Brown TR. Evaluation of manual methods for integration of in vivo phosphorus NMR spectra. NMR Biomed 1988;1:131–135.

80. Nelson SJ, Brown TR. A method for automatic quantification of one-dimensional spectra with low signal-to-noise ratio. J Magn Reson 1987;75:229–243.

81. Marshall I, Higinbotham J, Bruce S, Freise A. Use of Voigt lineshape for quantification of in vivo 1H spectra. Magn Reson Med 1997;37:651–657.

82. de Graaf AA, Bovee WM. Improved quantification of in vivo 1H NMR spectra by optimization of signal acquisition and processing and by incorporation of prior knowledge into the spectral fitting. Magn Reson Med 1990;15:305–319.

83. Vanhamme L, van den Boogaart A, Van Huffel S. Improved method for accurate and efficient quantification of MRS data with use of prior knowledge. J Magn Reson 1997;129:35–43.

84. Provencher SW. Estimation of metabolite concentrations from localized in vivo proton NMR spectra. Magn Reson Med 1993;30:672–679.

85. Ratiney H, Coenradie Y, Cavassila S, van Ormondt D, Graveron-Demilly D. Time-domain quantitation of 1H short echo-time signals: background accommodation. MAGMA 2004;16:284–296.

86. Govindaraju V, Young K, Maudsley AA. Proton NMR chemical shifts and coupling constants for brain metabolites. NMR Biomed 2000;13:129–153.

87. Young K, Govindaraju V, Soher BJ, Maudsley AA. Automated spectral analysis I: formation of a priori information by spectral simulation. Magn Reson Med 1998;40:812–815.

88. Graveron-Demilly D, Diop A, Briguet A, Fenet B. Product-operator algebra for strongly coupled spin systems. J Magn Reson A 1993;101:233–239.

89. Pfeuffer J, Tkac I, Provencher SW, Gruetter R. Toward an in vivo neurochemical profile: quantification of 18 metabolites in short-echo-time (1)H NMR spectra of the rat brain. J Magn Reson 1999;141:104–120.

90. Naressi A, Couturier C, Devos JM, et al. Java-based graphical user interface for the MRUI quantitation package. MAGMA 2001;12:141–152.

91. Slotboom J, Boesch C, Kreis R. Versatile frequency domain fitting using time domain models and prior knowledge. Magn Reson Med 1998;39:899–911.

92. in 't Zandt H, van Der Graaf M, Heerschap A. Common processing of in vivo MR spectra. NMR Biomed 2001;14:224–232.

93. Traber F, Block W, Lamerichs R, Gieseke J, Schild HH. 1H metabolite relaxation times at 3.0 tesla: measurements of T1 and T2 values in normal brain and determination of regional differences in transverse relaxation. J Magn Reson Imaging 2004;19:537–545.

94. Cavassila S, Deval S, Huegen C, van Ormondt D, Graveron-Demilly D. Cramer-Rao bounds: an evaluation tool for quantitation. NMR Biomed 2001;14:278–283.

95. Kreis R, Boesch C. Bad spectra can be better than good spectra [abstr]. In: Proceedings of the 11th Meeting of the International Society for Magnetic Resonance in Medicine. Berkeley, Calif: International Society for Magnetic Resonance in Medicine, 2003;264.

96. Behar KL, Ogino T. Characterization of macromolecule resonances in the 1H NMR spectrum of rat brain. Magn Reson Med 1993;30:38–44.

97. Hofmann L, Slotboom J, Boesch C, Kreis R. Characterization of the macromolecule baseline in localized (1)H-MR spectra of human brain. Magn Reson Med 2001;46:855–863.

98. Kassem MN, Bartha R. Quantitative proton short-echo-time LASER spectroscopy of normal human white matter and hippocampus at 4 tesla incorporating macromolecule subtraction. Magn Reson Med 2003;49:918–927.

99. Mader I, Seeger U, Weissert R, et al. Proton MR spectroscopy with metabolite-nulling reveals elevated macromolecules in acute multiple sclerosis. Brain 2001;124:953–961.

100. Hofmann L, Slotboom J, Jung B, Maloca P, Boesch C, Kreis R. Quantitative 1H-magnetic resonance spectroscopy of human brain: influence of composition and parameterization of the basis set in linear combi-

nation model-fitting. Magn Reson Med 2002;48:440–453.

101. Seeger U, Klose U, Mader I, Grodd W, Nagele T. Parameterized evaluation of macromolecules and lipids in proton MR spectroscopy of brain diseases. Magn Reson Med 2003;49:19–28.

102. Mader I, Seeger U, Karitzky J, Erb M, Schick F, Klose U. Proton magnetic resonance spectroscopy with metabolite nulling reveals regional differences of macromolecules in normal human brain. J Magn Reson Imaging 2002;16:538–546.

103. Graham GD, Hwang JH, Rothman DL, Prichard JW. Spectroscopic assessment of alterations in macromolecule and small-molecule metabolites in human brain after stroke. Stroke 2001;32:2797–2802.

104. Felblinger J, Kreis R, Boesch C. Effects of physiologic motion of the human brain upon quantitative 1H-MRS: analysis and correction by retro-gating. NMR Biomed 1998;11:107–114.

105. Haupt CI, Kiefer AP, Maudsley AA. In-plane motion correction for MR spectroscopic imaging. Magn Reson Med 1998;39:749–753.

106. Helms G, Piringer A. Restoration of motion-related signal loss and line-shape deterioration of proton MR spectra using the residual water as intrinsic reference. Magn Reson Med 2001;46:395–400.

107. de Graaf AA, van Dijk JE, Bovee WM. QUALITY: quantification improvement by converting lineshapes to the lorentzian type. Magn Reson Med 1990;13:343–357.

108. Klose U. In vivo proton spectroscopy in presence of eddy currents. Magn Reson Med 1990;14:26–30.

109. Hsu AC, Gregory CD. Offset-dependent partial saturation in binomial solvent suppression sequences. J Magn Reson 1998;131:46–53.

110. Marion D, Ikura M, Bax A. Improved solvent suppression in one- and two-dimensional NMR spectra by convolution of time-domain data. J Magn Reson 1989;84:425–430.

111. de Beer R, van Ormondt D. Analysis of NMR data using time domain fitting procedures. NMR Basic Princ Prog 1992;26:201–248.

112. Chang L, Cloak CC, Ernst T. Magnetic resonance spectroscopy studies of GABA in neuropsychiatric disorders. J Clin Psychiatry 2003;64(suppl 3):7–14.

113. Mueller SG, Trabesinger AH, Boesiger P, Wieser HG. Brain glutathione levels in patients with epilepsy measured by in vivo (1)H-MRS. Neurology 2001;57:1422–1427.

114. Trabesinger AH, Meier D, Boesiger P. In vivo 1H NMR spectroscopy of individual human brain metabolites at moderate field strengths. Magn Reson Imaging 2003;21:1295–1302.

115. Terpstra M, Henry PG, Gruetter R. Measurement of reduced glutathione (GSH) in human brain using LCModel analysis of difference-edited spectra. Magn Reson Med 2003;50:19–23.

116. Soher BJ, Young K, Govindaraju V, Maudsley AA. Automated spectral analysis III: application to in vivo proton MR spectroscopy and spectroscopic imaging. Magn Reson Med 1998;40:822–831.

117. Ebel A, Soher BJ, Maudsley AA. Assessment of 3D proton MR echo-planar spectroscopic imaging using automated spectral analysis. Magn Reson Med 2001;46:1072–1078.

118. Ernst RR, Bodenhausen G, Wokaun A. Principles of nuclear magnetic resonance in one and two dimensions. Oxford, England: Oxford University Press, 1987.

119. Hugg JW, Maudsley AA, Weiner MW, Matson GB. Comparison of k-space sampling schemes for multidimensional MR spectroscopic imaging. Magn Reson Med 1996;36:469–473.

120. Maudsley AA, Matson GB, Hugg JW, Weiner MW. Reduced phase encoding in spectroscopic imaging. Magn Reson Med 1994;31:645–651.

121. Kuhn B, Dreher W, Norris DG, Leibfritz D. Fast proton spectroscopic imaging employing k-space weighting achieved by variable repetition times. Magn Reson Med 1996;35:457–464.

122. Haupt CI, Schuff N, Weiner MW, Maudsley AA. Removal of lipid artifacts in 1H spectroscopic imaging by data extrapolation. Magn Reson Med 1996;35:678–687.

123. Chard DT, McLean MA, Parker GJ, MacManus DG, Miller DH. Reproducibility of in vivo metabolite quantification with proton magnetic resonance spectroscopic imaging. J Magn Reson Imaging 2002;15:219–225.

124. Wiedermann D, Schuff N, Matson GB, et al. Short echo time multislice proton magnetic resonance spectroscopic imaging in human brain: metabolite distributions and reliability. Magn Reson Imaging 2001;19:1073–1080.

125. Kreis R. Issues of spectral quality in clinical 1H-magnetic resonance spectroscopy and a gallery of artifacts. NMR Biomed 2004;17:361–381.

126. Natt O, Bezkorovaynyy V, Michaelis T, Frahm J. Use of phased array coils for a determination of absolute metabolite concentrations. Magn Reson Med 2005;53:3–8.

127. Srinivasan R, Vigneron D, Sailasuta N, Hurd R, Nelson S. A comparative study of myo-inositol quantification using LCmodel at 1.5 T and 3.0 T with 3 D 1H proton spectroscopic imaging of the human brain. Magn Reson Imaging 2004;22:523–528.